

A new double-line waveguide architecture for photonic applications using fs laser writing in Nd³⁺ doped GeO₂-PbO glasses

Camila D.S. Bordon^{a,*}, Jessica Dipold^b, Anderson Z. Freitas^b, Niklaus U. Wetter^b, Wagner de Rossi^b, Luciana R.P. Kassab^c

^a Departamento de Engenharia de Sistemas Eletrônicos, Escola Politécnica da USP, São Paulo, SP, Brazil

^b Centro de Lasers e Aplicações, Instituto de Pesquisas Energéticas e Nucleares, IPEN-CNEN, 2242, A. Prof. Lineu Prestes, São Paulo, SP, Brazil

^c Faculdade de Tecnologia de São Paulo, CEETEPS, São Paulo, SP, Brazil

ARTICLE INFO

Keywords:

fs laser processing
Germanate glasses
Double line waveguide
Active optical component

ABSTRACT

A new double-line waveguide architecture produced in Nd³⁺ doped GeO₂-PbO glasses is presented for photonic applications. The waveguides are written directly into Nd³⁺ doped GeO₂-PbO glasses using a Ti:Sapphire femtosecond (fs) laser, operating at 800 nm, delivering 30 fs pulses at 10 kHz repetition rate and writing speed of 0.5 mm/s. Two parallel lines form a dual-waveguide each line being a result of either 4 or 8 superimposed lines. Results of propagation losses, M² beam quality factor at 632 and 1064 nm, refractive index change, and relative gain at the signal wavelength (1064 nm) are presented. Structural changes, due to laser writing process were investigated by Raman spectroscopy. The observed near-field pattern image showed good waveguiding quality, consisting of a single, circular lobe. X,y-symmetrical guiding for both waveguides was observed. The relative gain reached 4.5 and 6.0 dB/cm for 4 and 8 superimposed lines, respectively, for 420 mW of 808 nm pumping. Propagation losses were 0.89 and 0.44 dB/cm, for 4 and 8 superimposed lines, respectively, leading to positive internal gain of 3.6 and 5.56 dB/cm. The results obtained in the present work demonstrate that this new double line architecture for Nd³⁺ doped GeO₂-PbO glasses is promising for the fabrication of integrated amplifiers, lossless components and lasers.

1. Introduction

The need to find suitable materials for integrated optics has led researchers to investigate different methods for waveguides fabrication. In particular, femtosecond (fs) laser processing of transparent dielectric materials appeared as a promising application not only for integrated optics [1], but also for integrated microsystems with optofluidic and mechanical characteristics in a single substrate (lab-on-a-chip) [2]. Two types of waveguides can be obtained in practice using the fs laser writing method: single or double-line. In the first type, the structural modification of the material causes a positive refractive index increase, leading to light confinement within the line [3]; in the second type, stress-induced negative refractive index changes occur in the laser focal region and light is guided in the pristine region between two or more written lines. In the present work we report results using the second type of writing for the production of the waveguides written directly in Nd³⁺ doped GeO₂-PbO glasses. Double-line waveguides demonstrated good results for undoped and Yb³⁺/Er³⁺ co-doped GeO₂-PbO glasses [4,5]

and motivated this investigation.

Initially, glass formers like silicates, borates, and phosphates were used as hosts for rare earth ions [6–9], followed by fluoride glasses, mainly because of their low phonon energy (500–600 cm⁻¹) [10–12]. However, their mechanical weakness and the necessity to use glove-box environment for their preparation led researchers to look for other alternatives. In this context, heavy metal oxide glasses appeared as another possible host [13–16] as they exhibit better thermal, mechanical and chemical durability, which allows them to be melted in ambient atmosphere, higher refractive index (~2.0) and low phonon energy (700–800 cm⁻¹). Several results of GeO₂-PbO glasses doped with rare-earth ions and metallic nanoparticles were reported and potential photonics applications demonstrated because of their enhanced linear and nonlinear optical properties. Here, the GeO₂-PbO glassy matrix was chosen due to prior experience and successful results the authors have obtained with this system. This host demonstrated to be an efficient material for optical amplifiers using Si technology [17], cover layers to enhance Si solar cell efficiency [18,19], and for sources for white light

* Corresponding author.

E-mail address: camiladvieira@gmail.com (C.D.S. Bordon).

generation and tunable visible light emission [20,21], among others.

We report a new strategy for the double-line configuration based on repeated collinear overlays of lines written at high speed when compared to previous work where a single line was written at a much slower speed [5]. Here, a nine times higher focal point displacement speed was used because a lower speed would lead to an accumulation of heat with consequent fracture of the glass due to the neodymium absorption at 800 nm that is in resonance with the fs laser's emitting wavelength. In order to maintain a high pulse overlap, which guarantees the intended effect of changing the refractive index, several lines were superimposed with a sufficiently long time interval between the writing of each line to allow for cooling of the affected region [5]. In this way, two parallel lines form a dual-waveguide, each line being the result of either 4 or 8 superimposed lines, which corresponds to a total local overlap of 576 or 1.152 pulses (considering a calculated diameter of 7.2 μm of the focal point inside the glass). Results of propagation losses, refractive index change, optical microscopy, absorbance measurements, M^2 beam quality factor (at 632 and 1064 nm), output mode profile, Raman spectroscopy and relative gain at 1064 nm are presented. The aim of this work is to verify the feasibility of the above outlined procedure and also to investigate optical amplification around 1064 nm, under 808 nm excitation. This new architecture can be extended to different hosts and represents an alternative usage of suitable materials for integrated optics.

2. Experimental

2.1. Preparation of the glasses

Glasses were obtained by the melt-quenching method with the addition of Nd_2O_3 (1.0 wt %) to the basic glass composition (in wt%): $40.0\text{GeO}_2 - 60.0\text{PbO}$. The reagents (with high purity of 99.999%) were melted in an alumina crucible for 1 h at 1200 °C, quenched in air in a preheated brass mold, and annealed at 420 °C for 1 h to avoid internal stress. The annealing is relevant to reduce the internal stress and provide less fragile samples as they may break during polishing. Finally, the samples were cut and polished to acquire optical quality surface. Transparent samples with thickness of 2 mm were produced.

2.2. Waveguide writing

The waveguide writing was performed using a femtosecond laser system (Ti:sapphire, model PRO 400, Femtolasers GmbH) with emission wavelength centered at 800 nm, pulse length of 30 fs, 200 μJ of maximum energy per pulse and 10 kHz repetition rate. During the writing process, the laser beam, with energy of 30 μJ per pulse, is focused perpendicular to the polished surface of the sample, with its linear polarization tilted 45° with respect to the movement direction and with the focal point positioned 0.75 mm below the surface. Two parallel lines separated by a distance of 10 μm were written. Each line itself was composed by 4 and 8 superimposed lines, as already described, written at a speed of 0.5 mm/s [22]. As explained before, the higher writing speed of 0.5 mm/s with respect to our previous work (0.06 mm/s) based on Yb/Er doped $\text{GeO}_2\text{-PbO}$ glass [5], was used in order to avoid the heating of the material because of the absorption of the Nd^{3+} doped $\text{GeO}_2\text{-PbO}$ material at 800 nm. After waveguide writing, the input and output facets of the samples were polished again to eliminate the surface damage suffered during femtosecond writing [4]. The final dimensions of the sample containing several waveguides was (5.18 \times 4.0 \times 2.0) mm^3 .

2.3. Characterization

The visible to near-infrared optical absorption spectrum was obtained at room temperature from 400 to 900 nm, using a commercial spectrophotometer (OceanOptics QE65 PRO), to verify the

incorporation of rare-earth ions. Raman spectroscopic measurements were made in the focal region using LabRam HR Evolution - HORIBA. Optical microscopy was performed using a Leica DMLP Polarizing Light Microscope with a MC170 HD camera.

The refractive index change was estimated by equation (1) (where n_1 and n_2 represent the refractive index of the core and the cladding, respectively) using the measured NA (numerical aperture) of the waveguide [22,23] as follows: the waveguide output beam diameter was measured at several distances and the numerical aperture of the waveguides was calculated from the ratio between the distance and the mode radius.

$$N.A. = \sqrt{n_1^2 - n_2^2} \approx \sqrt{2n_2\Delta n} \quad (1)$$

Propagation losses were determined at 1064 nm using the cut back method [24] and equation (2) where P_1 and P_2 represent the power corresponding to the different lengths of the samples, d_1 and d_2 , respectively, obtained with the experimental setup shown in Fig. 1.

$$\alpha [dB/cm] = -10 \frac{\log(P_2 - P_1)}{(d_2 - d_1)} \quad (2)$$

An experimental setup similar to the one shown in Fig. 1 was used to determine the near field profiles by using a CCD camera instead of the power meter and by changing the 10 \times objective to 20 \times and using a 632 nm laser. As reported in Ref. [22], this experimental setup was also used to determine the waveguide's NA.

The gain properties of the waveguides were characterized as follows: the relative gain (signal enhancement) was obtained by using two continuous (cw) laser diodes operating at 808 nm (maximum output power 420 mW) and 1064 nm for pump and signal wavelengths, respectively. The intensities of amplified spontaneous emission (ASE) and stimulated emission (SE) at 1064 nm were measured and the relative gain was determined using the experimental setup of Fig. 2. The relative gain measurements were carried out as follows: first, with the signal laser switched on and without the pump laser, the signal power was measured after propagation of the beam through the sample (P_{signal}). Signal input power was kept constant and at very low level (400 nW) to avoid gain saturation. Then, the measurement was repeated with both lasers (pump and signal) turned on ($P_{\text{signal+ASE}}$) and the SE and ASE at 1064 nm were recorded together. Finally, ASE was measured (P_{ASE}) by turning the signal off and leaving the pump on; then the relative gain was determined from the following equation (3) where $d = 0.5$ cm represents the sample length [5,17,24–26]:

$$G \left[\frac{dB}{cm} \right] = \frac{10 \times \log((P_{\text{signal+ASE}} - P_{\text{ASE}}) / P_{\text{signal}})}{d} \quad (3)$$

3. Results and discussion

3.1. Optical and Raman spectroscopy results

Linear absorption measurements of the polished glasses after the fabrication process demonstrated transparent and homogeneous samples, as shown in Fig. 3. The observed spectra highlights the typical absorption of Nd^{3+} doped glasses and demonstrates the presence of the rare-earth ions in trivalent form, which are responsible for lasing action. Images obtained from optical microscopy can be seen in Fig. 4. A top view image of double waveguides written in Nd^{3+} doped $\text{GeO}_2\text{-PbO}$ glass with 8 superimposed lines (pulse energy of 30 μJ , writing speed of 0.5 mm/s) is presented; the distance between the pair of parallel lines is 10 μm .

Raman results are presented in Fig. 5 for the bulk glass without waveguides (Fig. 5a) and 5b shows the results obtained between the two lines written with 8 superimposed lines, which shows no change. This fact suggests that our fs laser writing procedure causes no fundamental structural change in the guiding region between the two lines, as

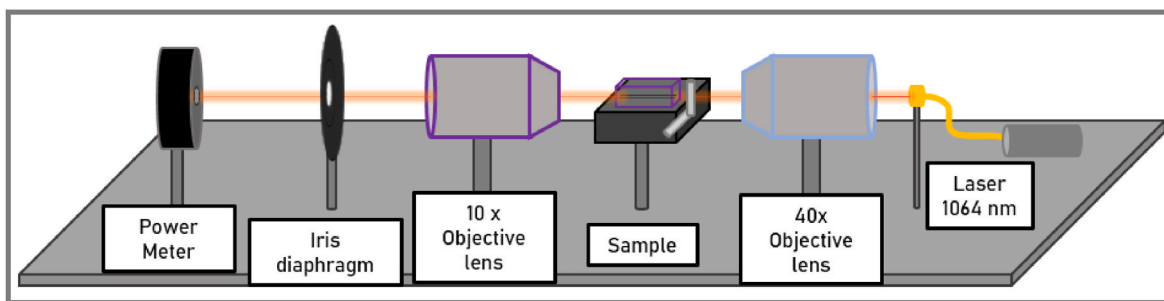


Fig. 1. Experimental setup used for the measurements of the propagation losses.

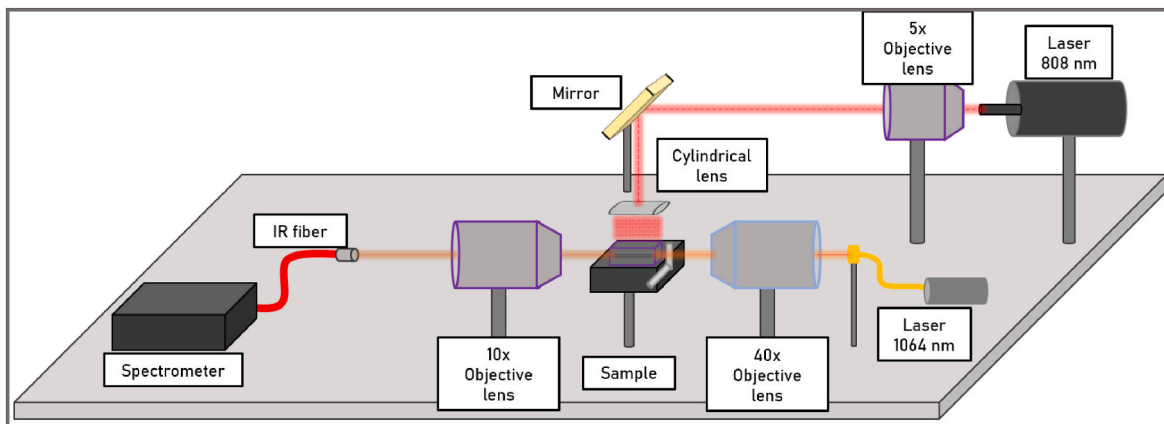


Fig. 2. Experimental setup used for relative gain measurements at 1064 nm (excitation at 808 nm).

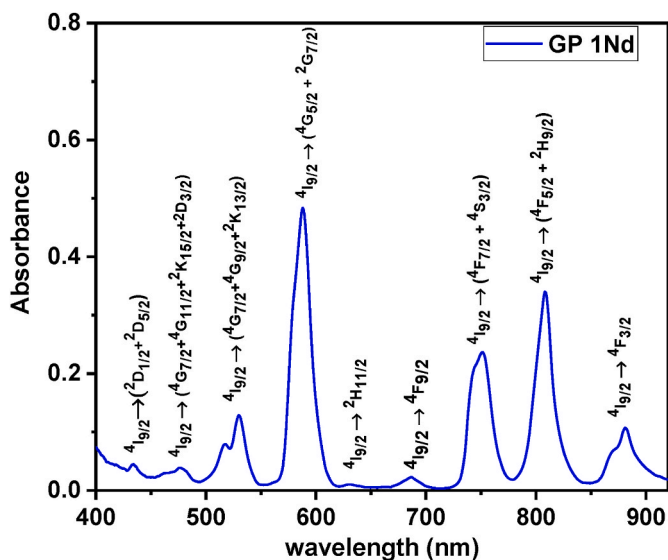


Fig. 3. Absorbance results for Nd^{3+} doped $\text{GeO}_2\text{-PbO}$ glass at room temperature.

reported before [4,5]. Comparing these results of Fig. 5a and b with Fig. 5c that shows the Raman spectrum taken in the center of one of the lines (written with 8 superimposed lines) we observe the following changes: The peak at 347.8 cm^{-1} (bulk) shifts to 356.6 cm^{-1} (written region) and indicates that the laser writing process changes the Ge-O-Ge bending mode's vibrational frequency [4,27]. The same applies to the peak at 439.7 cm^{-1} (bulk) that shifts to 446.2 cm^{-1} (written region) and demonstrates that symmetric stretching vibrations of the Ge-O-Ge bonds are altered with the laser writing process. The shift of the peak at 515.5

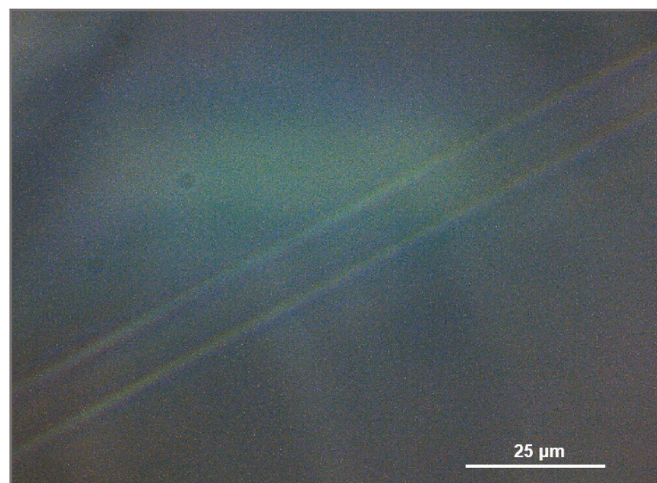


Fig. 4. Top view microscope image of a double-line waveguide written in Nd^{3+} doped $\text{GeO}_2\text{-PbO}$ glass with 8 superimposed lines; the distance between the pair of parallel lines is $10\text{ }\mu\text{m}$. (pulse energy of $30\text{ }\mu\text{J}$, writing speed of 0.5 mm/s).

cm^{-1} (bulk) to 510.1 cm^{-1} (written region), relates to symmetric stretching vibrations along the Ge-O-Ge chain [4,27] and indicates a different density of these type of bonds in the written region, as reported in a previous work of undoped $\text{GeO}_2\text{-PbO}$ glass, in which the writing process was different, as the double lines were not formed by superimposed lines as in the present study [4]. The peaks at 774 cm^{-1} (bulk) and 772 cm^{-1} (inside line) and at 863 cm^{-1} (bulk) and 861 cm^{-1} (written region), that correspond to Ge-O and Ge-O-Ge symmetric stretching vibrations in the GeO_4 tetrahedral units [4,27], and asymmetric stretching vibrations of Ge-O-Ge bonds, respectively, change only

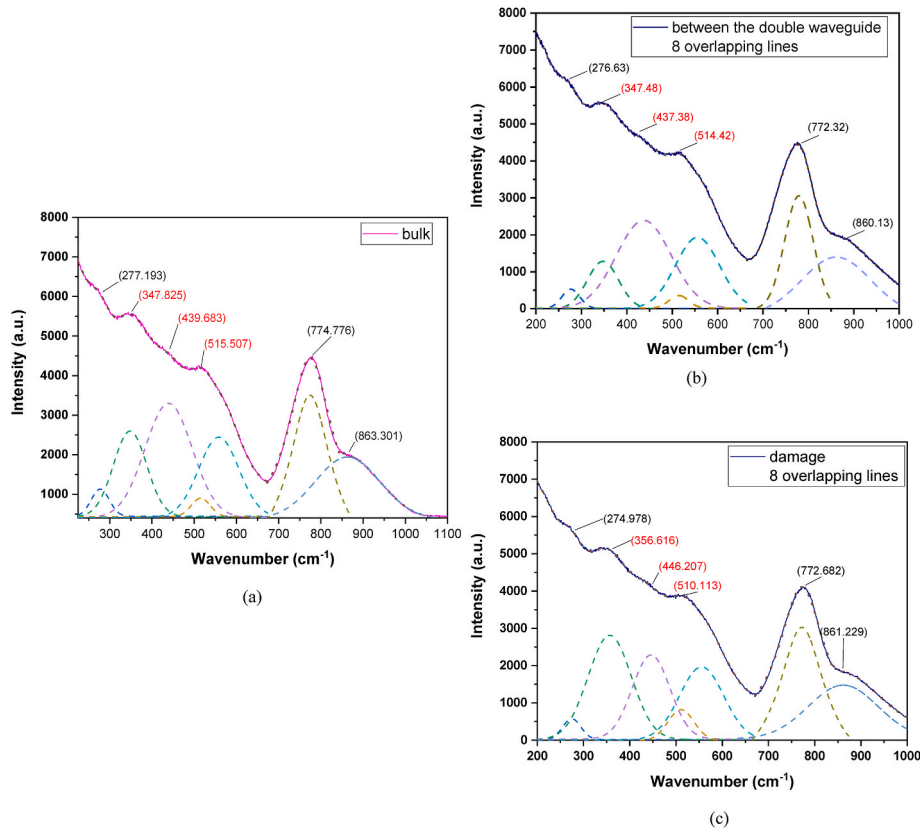


Fig. 5. Raman results of Nd^{3+} doped $\text{GeO}_2\text{-PbO}$ glass in a) the bulk area and b) between the double waveguide written with 8 superimposed lines. c) Raman results inside one of the fs written lines of the double waveguide written with 8 superimposed lines.

slightly, showing little influence of the laser writing process. Similar changes observed in the Raman spectra related to laser-induced alteration of the structure have been observed in other glasses [28,29].

3.2. Passive and active characterization results

Table 1 presents the results of Δn_x and Δn_y at 632 nm. We observe that the created index change is negative in the center of the written lines. As a result, the unchanged guiding region between both written lines shows a positive index difference when compared to the center of the written lines. Similar values are obtained for both directions: $\Delta n_x = 5.7 \times 10^{-3}$, $\Delta n_y = 5.4 \times 10^{-3}$ and $\Delta n_x = 7.3 \times 10^{-3}$, $\Delta n_y = 5.3 \times 10^{-3}$ for double waveguides written with 4 and 8 superimposed lines, respectively. The results of the beam quality factor (M^2), at 632 and 1064 nm, determined using standard procedures as already reported [22,30], are also shown, indicating a x,y-symmetrical guiding for both waveguides (4 and 8 superimposed lines). Low propagation loss values were obtained: 0.89 and 0.44 dB/cm for 4 and 8 superimposed lines, respectively. Near field mode profiles at 632 nm, are presented in Fig. 6

Table 1

Results of index difference (Δn), M_x^2 and M_y^2 and propagations losses (pulse energy of 30 μJ and writing speed of 0.5 mm/s).

PARAMETERS	4 SUPERIMPOSED LINES	8 SUPERIMPOSED LINES
Δn_x	5.7×10^{-3}	7.3×10^{-3}
Δn_y	5.4×10^{-3}	5.3×10^{-3}
M_x^2 (at 632 nm)	16.7	16.6
M_y^2 (at 632 nm)	14.2	15.6
M_x^2 (at 1064 nm)	9.9	9.9
M_y^2 (at 1064 nm)	8.4	9.2
Propagation losses (dB/cm)	0.89	0.44

for waveguides written with 4 and 8 superimposed lines and demonstrate the presence of confined beams that correspond to single transverse mode.

Fig. 7a and b shows the variation of the relative gain at 1064 nm as a function of the pump power (808 nm) for 400 nW of input signal power for the double waveguides, determined using equation (3). Fig. 8 presents the ASE spectrum without signal for 184 mW of pump power and the amplified signal after ASE removal using 400 nW of input signal strength at 1064 nm. The relative gain reached 4.5 and 6.0 dB/cm for 4 and 8 superimposed lines, respectively, for 420 mW of 808 nm pump power, after which point saturation takes place. We highlight a larger relative gain for the waveguide written with 8 superimposed lines. If we take into account propagation losses (α) presented in Table 1, the internal gain can be calculated as in Refs. [5,24]. Considering the propagation losses (Table 1) of 0.89 and 0.44 dB/cm at 1064 nm, for 4 and 8 superimposed lines, respectively, we can calculate the internal gain for 420 mW of pump power by $G_{\text{INT}} = G_{\text{R}} - \alpha$ and a positive internal gain of 3.61 and 5.56 dB/cm is obtained for 4 and 8 superimposed lines, respectively. Consequently, we come to the conclusion that the waveguides written with 8 superimposed lines represent a better condition for optical amplifiers applications at 1064 nm.

4. Conclusion

This work presents double-line waveguide amplifiers in Nd^{3+} doped $\text{GeO}_2\text{-PbO}$ glasses produced by direct fs laser writing using a new technique based on several superimposed lines. Samples were prepared using a standard melt-quenching technique that allowed the production of optical-quality glasses. Absorption measurements confirmed the incorporation of the trivalent form of the rare-earth ions. The waveguides were written using 30 fs, 800 nm laser pulses, and either 4 or 8 superimposed lines. The refractive index difference at the center of the

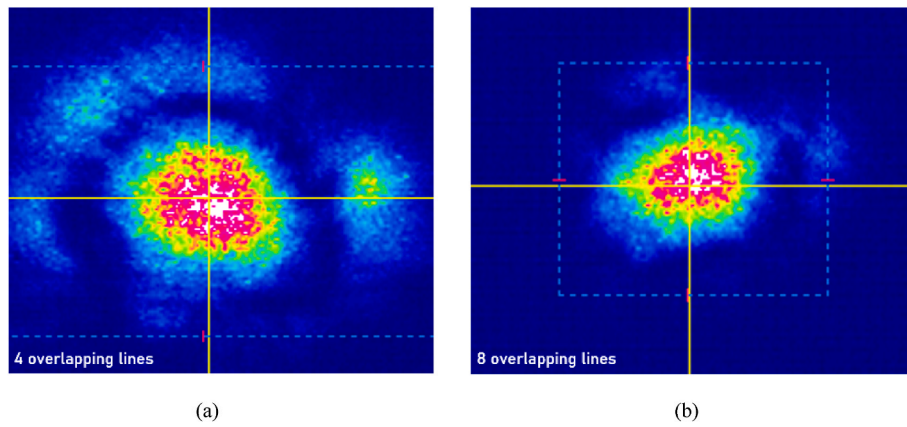


Fig. 6. Beam images (at 632 nm) from the double waveguides for (a) 4 and (b) 8 superimposed lines.

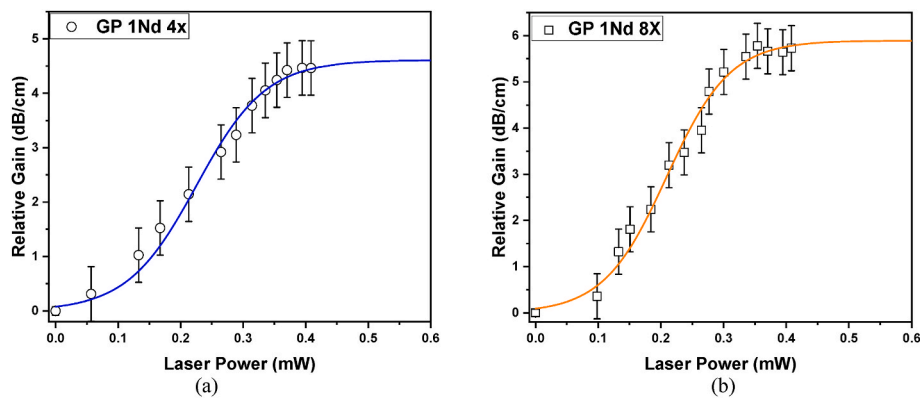


Fig. 7. Relative gain (signal enhancement) at 1064 nm as a function of pump power at 808 nm for 400 nW of input signal power for the dual waveguides written in Nd^{3+} doped $\text{GeO}_2\text{-PbO}$ with a) 4 superimposed and b) 8 superimposed lines.

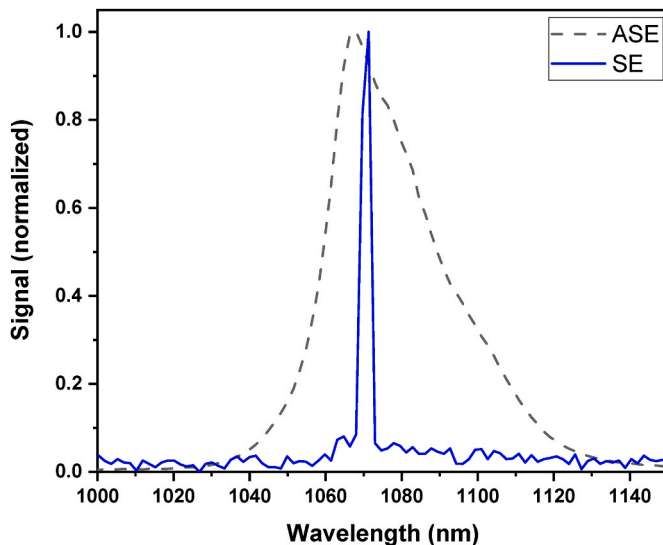


Fig. 8. Normalized ASE spectrum without signal for 184 mW of pump power at 808 nm (dashed line) and the signal at the waveguide output after ASE removal (SE) using 400 nW of input signal power at 1064 nm (solid line) for 8 superimposed lines.

waveguide was $6.3 (\pm 1.0) \times 10^{-3}$ in both directions and for both waveguides. The observed near-field pattern image showed good waveguiding quality, consisting of a single, circular lobe. X,y-symmetrical

guiding for both waveguides was observed. Propagation losses were 0.89 and 0.44 dB/cm for 4 and 8 superimposed lines, respectively. The best condition for amplification was achieved by waveguides written with 0.5 mm/s and 30 μJ with 8 superimposed lines resulting in a relative gain of 6.0 dB/cm for 420 mW of pump power at 808 nm. We highlight that a positive internal gain of 3.61 and 5.56 dB/cm was obtained for 4 and 8 superimposed lines, respectively. The results obtained in the present work demonstrate that this new double line architecture for Nd^{3+} doped $\text{GeO}_2\text{-PbO}$ glasses is promising for the fabrication of integrated amplifiers, lossless components and lasers. Moreover, it can be extended to different hosts to operate in different regions of the telecom bands.

Declaration of competing interest

The authors declare that they have no known competing financial interests or personal relationships that could have appeared to influence the work reported in this paper.

Acknowledgments

We acknowledge financial support from Fundação de Amparo à Pesquisa do Estado de São Paulo (FAPESP) (2019/06334-4, 2016/02326-9, 2017/10765-5 and 2013/26113-6, EMU 2018/19240-5, 2017/50332-0) and from Conselho Nacional de Desenvolvimento Científico e Tecnológico - Grant: INCT/CNPq 465.763/2014 (Instituto Nacional de Ciência e Tecnologia de Fotônica), Grant: 302532/2019-6, and Grant: SISFÓTON-MCTI 440228/2021-2 (Sistema Nacional de Laboratórios de Fotônica).

References

- [1] S. Nolte, M. Wil, J. Burghoff, A. Tuennermann, Femtosecond waveguide writing: a new avenue to three-dimensional integrated optics, *Appl. Phys. Mater. Sci. Process* 77 (2003) 109–111, <https://doi.org/10.1007/s00339-003-2088-6>.
- [2] F. Sima, K. Sugioka, R.M. Vázquez, R. Osellame, L. Kelemen, P. Ormos, Three-dimensional femtosecond laser processing for lab-on-chip applications, *Nanophotonics* 7 (2018) 613–634, <https://doi.org/10.1515/nanoph-2017-0097>.
- [3] D. Homoele, S. Wielandy, A.L. Gaeta, N.F. Borrelli, C. Smith, Infrared photosensitivity in silica glasses exposed to femtosecond laser pulses, *Opt. Lett.* 24 (1999) 1311–1313, <https://doi.org/10.1364/OL.24.001311>.
- [4] D.S. da Silva, N.U. Wetter, W. de Rossi, L.R.P. Kassab, R.E. Samad, Production and characterization of femtosecond laser-written double line waveguides in heavy metal oxide glasses, *Opt. Mater.* 75 (2018) 267–273, <https://doi.org/10.1016/j.optmat.2017.10.033>.
- [5] D.S. Da Silva, N.U. Wetter, L.R.P. Kassab, W. De Rossi, M.S. De Araujo, Double line waveguide amplifiers written by femtosecond laser irradiation in rare-earth doped germanate glasses, *J. Lumin.* 217 (2020) 116789, <https://doi.org/10.1016/j.jlumin.2019.116789>.
- [6] H. Lin, E.Y.B. Pun, X. Wang, X. Liu, Intense visible fluorescence and energy transfer in Dy^{3+} , Tb^{3+} , Sm^{3+} and Eu^{3+} doped rare-earth borate glasses, *J. Alloys Compd.* 390 (2005) 197–201, <https://doi.org/10.1016/j.jallcom.2004.07.068>.
- [7] Y. Nageno, H. Takebe, K. Morinaga, Correlation between radiative transition probabilities of Nd^{3+} and composition in silicate, borate, and phosphate glasses, *J. Am. Ceram. Soc.* 76 (1993) 3081–3086, <https://doi.org/10.1111/j.1151-2916.1993.tb06612.x>.
- [8] K. Pátek, in: J.G. Edwards (Ed.), *Glass Lasers*, Butterworth, England, 1970.
- [9] S. Tanabe, S. Ohyagi, N. Soga, T. Hanada, Compositional dependence of Judd-Ofelt parameters of Er^{3+} ions in alkali-metal borate glasses, *Phys. Rev. B* 46 (1992) 3305, <https://doi.org/10.1103/PhysRevB.46.3305>.
- [10] P.W. France, P.W. France, M.G. Drexhage, J.M. Parker, M.W. Moore, S.F. Carter, in: J.V. Wright (Ed.), *Fluoride Glass Optical Fibers*, Blackie, Glasgow, 1990.
- [11] S. Nishibu, S. Yonezawa, M. Takashima, Preparation and optical properties of $\text{HoF}_3\text{-BaF}_2\text{-AlF}_3\text{-GeO}_2$ glasses, *J. Non-Cryst. Solids* 351 (2005) 1239–1245, <https://doi.org/10.1016/j.jnoncrysol.2005.03.017>.
- [12] A. Flórez, E.M. Ulloa, R. Cabanzo, Optical properties of Nd^{3+} and Er^{3+} ions in fluoro-phosphate glasses: effects of P_2O_5 concentration and laser applications, *J. Alloys Compd.* 488 (2009) 606–611, <https://doi.org/10.1016/j.jallcom.2009.09.046>.
- [13] W.R. Dumbaugh, Heavy metal oxide glasses containing Bi_2O_3 , *Phys. Chem. Glasses* 27 (1986) 119–123.
- [14] P. Nachimuthu, M. Vithal, R. Jagannathan, Absorption and emission spectral properties of Pr^{3+} , Nd^{3+} , and Eu^{3+} ions in heavy-metal oxide glasses, *J. Am. Ceram. Soc.* 83 (2000) 597–604, <https://doi.org/10.1111/j.1151-2916.2000.tb01238.x>.
- [15] W.A. Pisarski, J. Pisarska, G. Dominiak-Dzik, M. Mączka, W. Ryba-Romanowski, Compositional-dependent lead borate based glasses doped with Eu^{3+} ions: synthesis and spectroscopic properties, *J. Phys. Chem. Solid.* 67 (2006) 2452–2457, <https://doi.org/10.1016/j.jpcs.2006.06.022>.
- [16] H. Lin, S. Tanabe, L. Lin, Y.Y. Hou, K. Lin, D.L. Yang, T.C. Ma, J.Y. Yu, E.Y.B. Pun, Near-infrared emissions with widely different widths in two kinds of Er^{3+} -doped oxide glasses with high refractive indices and low phonon energies, *J. Lumin.* 124 (2007) 167–172, <https://doi.org/10.1016/j.jlumin.2006.02.019>.
- [17] F.A. Bomfim, R.C. Rangel, D.M. da Silva, D.O. Carvalho, E.G. Melo, M.I. Alayo, L.R. P. Kassab, A new fabrication process of pedestal waveguides based on metal dielectric composites of $\text{Yb}^{3+}/\text{Er}^{3+}$ codoped PbO-GeO_2 thin films with gold nanoparticles, *Opt. Mater.* 86 (2018) 433–440, <https://doi.org/10.1016/j.optmat.2018.10.044>.
- [18] R.M. Gunji, E.D.A. Santos, C.D.S. Bordon, J.A.M. Garcia, L.A. Gómez-Malagón, L.R. P. Kassab, Germanate glass layer containing Eu^{3+} ions and gold nanoparticles for enhanced silicon solar cell performance, *J. Lumin.* 226 (2020) 117497, <https://doi.org/10.1016/j.jlumin.2020.117497>.
- [19] R.M. Gunji, G.R.S. Mattos, C.D.S. Bordon, L.A. Gómez-Malagón, L.R.P. Kassab, Efficiency enhancement of silicon solar cells covered by $\text{GeO}_2\text{-PbO}$ glasses doped with Eu^{3+} and TiO_2 nanoparticles, *J. Lumin.* 223 (2020) 117244, <https://doi.org/10.1016/j.jlumin.2020.117244>.
- [20] M.E. Camilo, E.D.O. Silva, L.R.P. Kassab, J.A.M. Garcia, C.B. De Araújo, White light generation controlled by changing the concentration of silver nanoparticles hosted by $\text{Ho}^{3+}/\text{Tm}^{3+}/\text{Yb}^{3+}$ doped $\text{GeO}_2\text{-PbO}$ glasses, *J. Alloys Compd.* 644 (2015) 155–158, <https://doi.org/10.1016/j.jallcom.2015.04.108>.
- [21] L.R.P. Kassab, C.D.S. Bordon, A.S. Reyna, C.B. de Araújo, Nanoparticles-based photonic metal–dielectric composites: a survey of recent results, *Opt. Mater.* X 12 (2021) 100098, <https://doi.org/10.1016/j.omx.2021.100098>.
- [22] C.D.S. Bordon, N.U. Wetter, W. de Rossi, L.P.R. Kassab, Fs laser writing in Nd^{3+} doped $\text{GeO}_2\text{-PbO}$ glasses for the production of a new double line waveguide architectures for photonic applications, *Proc. SPIE* (2022), <https://doi.org/10.1117/12.2610155>, 12004, 120040Y-120041Y- 120040Y-120046Y.
- [23] R.R. Gattass, E. Mazur, Femtosecond laser micromachining in transparent materials, *Nat. Photonics* 2 (2008) 219–225, <https://doi.org/10.1038/nphoton.2008.47>.
- [24] D.L. Yang, E.Y.B. Pun, B.J. Chen, H. Lin, Radiative transitions and optical gain in $\text{Er}^{3+}/\text{Yb}^{3+}$ codoped acid-resistant ion exchanged germanate glass channel waveguides, *J. Opt. Soc. Am. B* 26 (2009) 357–363, <https://doi.org/10.1364/JOSAB.26.000357>.
- [25] M.M. Martins, L.R.P. Kassab, D.M. da Silva, C.B. de Araújo, Tm^{3+} doped $\text{Bi}_2\text{O}_3\text{-GeO}_2$ glasses with silver nanoparticles for optical amplifiers in the short-wave-infrared-region, *J. Alloys Compd.* 772 (2018) 58–63, <https://doi.org/10.1016/j.jallcom.2018.08.146>.
- [26] C.D.S. Bordon, E.S. Magalhaes, D.M. da Silva, L.R.P. Kassab, C.B. de Araújo, Influence of Al_2O_3 on the photoluminescence and optical gain performance of Nd^{3+} doped germanate and tellurite glasses, *Opt. Mater.* 109 (2020) 110342, <https://doi.org/10.1016/j.optmat.2020.110342>.
- [27] R.C. Lucacel, C. Marcus, I. Ardelean, FTIR and Raman spectroscopic studies of copper doped $2\text{GeO}_2\text{-PbO-Ag}_2\text{O}$ glasses, *J. Optoelectron. Adv. Mater.* 9 (2007) 747–750.
- [28] T.T. Fernandez, M. Hernandez, B. Sotillo, S.M. Eaton, G. Jose, R. Osellame, A. Jha, P. Fernandez, J. Solis, Role of ion migrations in ultrafast laser written tellurite glass waveguides, *Opt Express* 22 (2014) 15298–15304, <https://doi.org/10.1364/OE.22.015298>.
- [29] B. Sotillo, A. Chiappini, V. Bharadwaj, M. Ramos, T.T. Fernandez, S. Rampini, M. Ferrari, R. Ramponi, P. Fernandez, B. Gholipour, C. Soci, S.M. Eaton, Raman spectroscopy of femtosecond laser written low propagation loss optical waveguides in Schott N-SF8 glass, *Opt. Mater.* 62 (2017) 626–631, <https://doi.org/10.1016/j.optmat.2017.07.002>.
- [30] D. Feise, G. Blume, H. Dittrich, C. Kaspari, K. Paschke, G. Erbert, High-brightness 635nm tapered diode lasers with optimized index guiding, *Proc. SPIE* 7583 (2010), <https://doi.org/10.1117/12.840658>, 75830V-1-75830V-12.